

# EchoMimicV3: 1.3B Parameters are All You Need for Unified Multi-Modal and Multi-Task Human Animation

Rang Meng Yan Wang Weipeng Wu Ruobing Zheng Yuming Li<sup>‡</sup> Chenguang Ma<sup>‡</sup>

Terminal Technology Department, Alipay, Ant Group  
{mengrang.mr, luoque.lym, chenguang.mcg}@antgroup.com

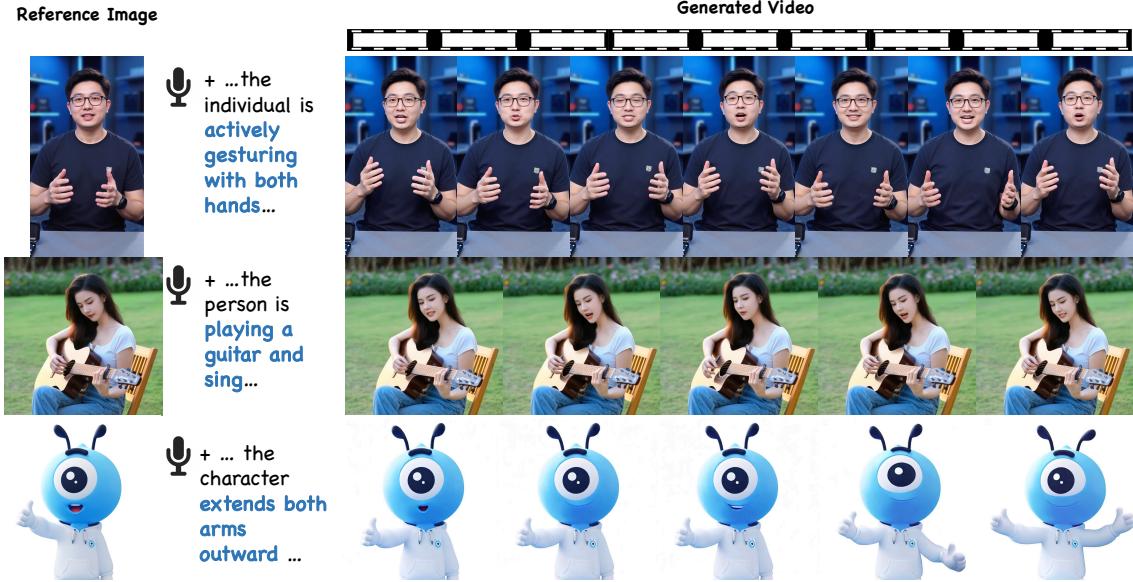


Figure 1: EchoMimicV3, an efficient framework with just 1.3B parameters for unified Multi-Modal and Multi-Task human video generation. Based on the audio, prompt and reference image over various scenes, EchoMimicV3 generate a video where lip movements and facial expression align with the audio, and the gestures and scene follow the prompt.

## Abstract

Human animation recently has advanced rapidly, achieving increasingly realistic and vivid results, especially with the integration of large-scale video generation models. However, the slow inference speed and high computational cost of these large models bring significant challenges for practical applications. Additionally, various tasks in human animation, such as lip-syncing, audio-driven full-body animation, and video generation from start and end frames, often require different specialized models. The introduction of large video models has not alleviated this dilemma. This raises an important question: Can we make human animation **Faster, Higher** in quality, **Stronger** in generalization, and make various tasks **Together** in one model? To address this, we dive into video generation models and discover that the devil lies in the details: 1) Inspired by MAE, we propose a novel unified Multi-Task paradigm for human animation, treating diverse generation tasks as spatial-temporal local reconstructions, requiring modifications only on the input side; 2) Given the in-

terplay and division among multi-modal conditions including text, image, and audio, we introduce a multi-modal decoupled cross-attention module to fuse multi-modals in a divide-and-conquer manner; 3) We propose a new SFT+Reward alternating training paradigm, enabling the minimal model with 1.3B parameters to achieve generation quality comparable to models with 10 times the parameters count. Through these innovations, our work paves the way for efficient, high-quality, and versatile digital human generation, addressing both performance and practicality challenges in the field. Extensive experiments demonstrate that EchoMimicV3 outperforms existing models in both facial and semi-body video generation, providing precise text-based control for creating videos in a wide range of scenarios, such as podcasts, karaoke, dynamic scenes, multi-aspect ratios, and so on. We commit to open-sourcing our code.

## Introduction

*“Faster, Higher, Stronger – Together”*

— The Olympic Motto

<sup>‡</sup> Corresponding author

In recent years, human animation has made remarkable progress, generating highly realistic and lifelike human videos. The advancement is also largely driven by the integration of large video generation models. However, these models face significant challenges: 1) their inference speeds are often slow, and they demand high computational resources. 2) Additionally, different tasks in human animation are often handled separately. For instance, lip-syncing relies on one model. Audio-driven full-body motion depends on another. Video synthesis from sparse frames requires yet another model. The emergence of large video models has not resolved this issue.

This raises a critical question: Can we create a single model that needs to be Faster and produce Higher-quality human videos, and it should also generalize stronger and handle multiple tasks simultaneously. To answer this problem, we explored video generation models and uncovered key insights.

First, inspired by MAE, we propose a unified multi-task framework for human animation. This framework treats various generation tasks as spatial-temporal local reconstructions. It only requires changes on the input side, simplifying the process. Second, considering the complex interactions among text, image, and audio modalities, we introduced a multi-modal decoupled cross-attention module. This module fuses different modalities in a divide-and-conquer manner. Consequently, it improves both efficiency and accuracy. Finally, we developed a novel SFT+Reward alternating training strategy. This strategy enables a compact model with 1.3B parameters to match the performance of much larger models. These larger models often have 10 times the parameters.

Our work bridges the gap between performance and practicality in digital human generation. Through extensive experiments, we demonstrated that EchoMimicV3 surpasses existing methods. It excels in both facial and semi-body video generation. Furthermore, it offers precise text-based control. This makes it versatile for diverse scenarios. For example, it can be used in podcasts, karaoke, dynamic scenes, and videos with varying aspect ratios. We are committed to open-sourcing our code. By doing so, we aim to foster further research and innovation.

Moreover, the current state of human animation is highly fragmented. Lip-syncing relies on one model, while audio-driven full-body motion depends on another. Similarly, video synthesis from sparse frames uses yet another model. This reliance on specialized models complicates the development of unified solutions. Therefore, there is a clear need for a more integrated approach. Our proposed framework addresses this fragmentation. It paves the way for efficient and versatile human animation systems.

In summary, our contributions are as follows:

- We propose a unified Multi-Task human animation framework, treating various generation tasks as spatial-temporal local reconstructions and making diverse tasks together in a single model.
- Our Multi-Modal Decoupled Cross-attention module can facilitate cross-modal interaction among vision, text, and

audio while retaining their unique representations.

- Our alternative SFT and DPO training strategy can empower the minimal model with the capabilities of 10 times larger scale models to generate vivid talking human videos for diverse scenarios.
- Our method demonstrates strong competitiveness when compared to other models with ten times the parameter count, through both quantitative and qualitative experiments.

## EchoMimicV3

EchoMimicV3 aims to create talking human videos with vivid gestures and natural body movements, with conditions of the reference image, audio, and text prompt, without cumbersome conditions such as predefined 2D or 3D poses. The pipeline of EchoMimicV3 is illustrated in Fig. 2. To unify diverse tasks, we utilize the Multi-Task Coupled Masked Inpainting module (Sec 3.2). Additionally, to enhance the generative capabilities of  $\sim 1\text{B}$  models, we propose a novel training strategy that alternates between Supervised Fine-Tuning (SFT) and Direct Preference Optimization (DPO) (Sec 3.3). To facilitate cross-modal interaction among vision, text, and audio while retaining their unique representations, we present Multi-Modal Decoupled Cross Attention (Sec 3.4).

### Preliminaries

**Latent Diffusion Model.** Latent Diffusion Model (LDM) (Rombach et al. 2022) leverages a Variational Autoencoder (VAE) Encoder (Kingma 2013)  $E$  to project an image  $I$  from pixel space into a more compact latent representation, denoted as  $z_0 = E(I)$ . During the training phase, Gaussian noise is incrementally injected into the latent code  $z_0$  over a sequence of timesteps  $t \in [1, \dots, T]$ . This process ensures that the final noisy latent representation  $z_T$  converges to a standard normal distribution  $\mathcal{N}(0, 1)$ . The core objective of LDM is to learn a denoising function that can accurately estimate the noise added at each timestep  $t$ . The training loss is formulated as follows:

$$L_{\text{latent}} = \mathbb{E}_{z_t, t, c, \epsilon \sim \mathcal{N}(0, 1)} [\|\epsilon - \epsilon_\theta(z_t, t, c)\|_2^2], \quad (1)$$

where  $\epsilon_\theta$  denotes a trainable Denoising U-Net that predicts the noise component, and  $c$  represents conditional information such as text prompts or audio signals that guide the generation process. By incorporating these conditions, the model gains the ability to generate highly diverse and contextually relevant outputs.

During inference, the pretrained model iteratively refines a latent vector sampled from the Gaussian distribution  $\mathcal{N}(0, 1)$ . At each step, the model removes the estimated noise, gradually transforming the random latent vector into a meaningful representation. Finally, the denoised latent code is decoded back into the pixel space using the VAE decoder  $D$ , yielding the generated image. This two-stage approach—operating in the latent space followed by decoding—ensures both efficiency and high-quality generation. By performing diffusion in the latent space instead of the pixel space, the model avoids the prohibitive computational

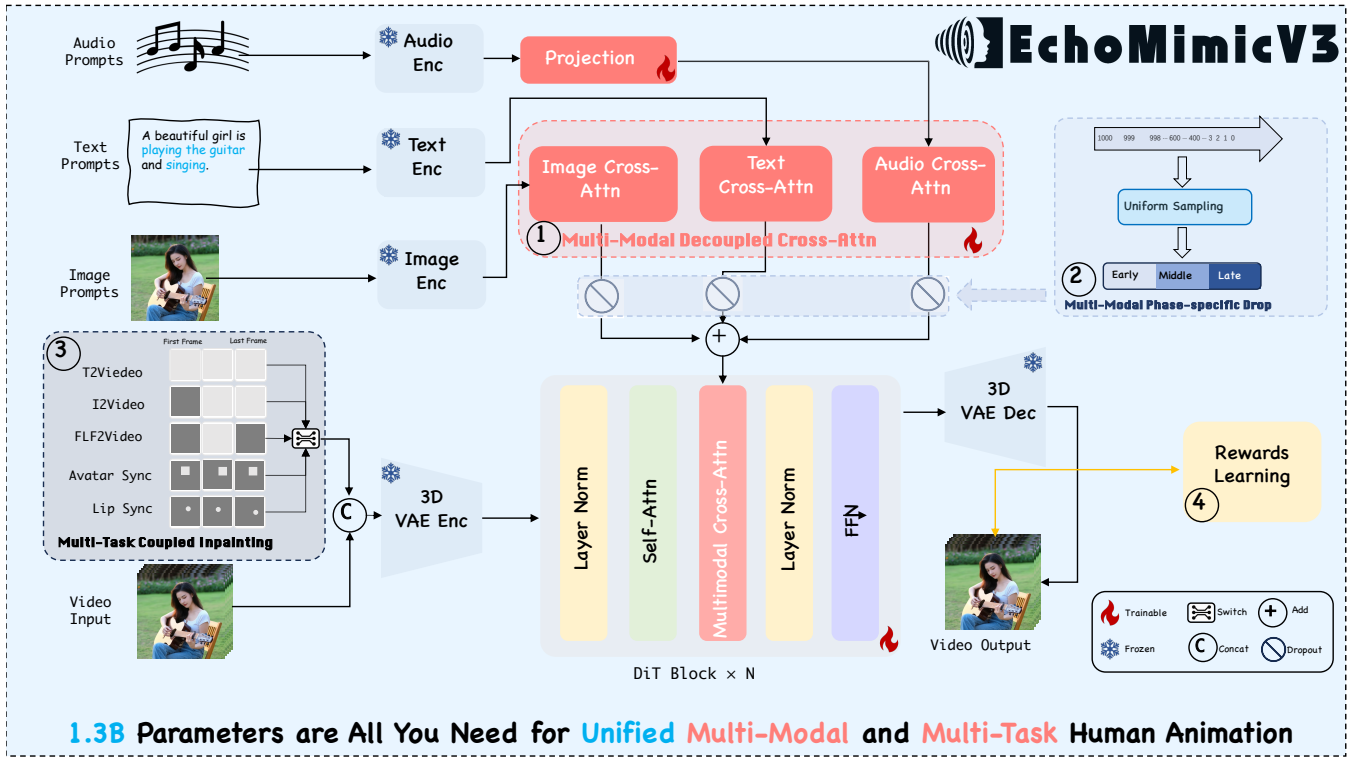


Figure 2: The overview of EchoMimicV3.

costs with high-resolution image generation. Additionally, the use of conditional inputs  $c$  enables fine-grained control over the generation process, making it suitable for a wide range of applications, including text-to-image synthesis, image inpainting, and style transfer.

**Diffusion Transformers.** Diffusion Transformers (DiT) (Peebles and Xie 2023) presents a significant advancement over traditional diffusion models by applying transformer-based architectures (Vaswani et al. 2017) into the denoising process. Unlike conventional approaches that rely on convolutional layers, DiT leverages self-attention mechanisms to capture non-local dependencies in high-dimensional data, making it particularly effective for tasks involving long video sequences or complex spatial-temporal patterns. By employing a fully attention-driven transformer architecture operating in the latent space, DiT enhances the model’s ability to produce high-fidelity and temporally consistent video outputs, which are critical for applications such as human video generation.

### Multi-Task Coupled Mask Inpainting

The WAN video model not only incorporates video latent at the DiT input, but also includes a corresponding 0-1 sequence of the same length. For the I2V task, this 0-1 sequence assigns a value of 1 to the first frame and 0 to all subsequent frames, effectively masking the video input while designating the first frame as the reference image. This masked sequence is then concatenated with the video latent before being fed into the DiT. Inspired by MAE, we fully leverage the 0-1 masking module to estab-

lish a unified paradigm for various human animation tasks. Specifically, we treat first-frame as reference, first-and-last-frame reference, and mouth replacement as post-first-frame sequence reconstruction, inter-first-and-last-frame sequence reconstruction, and local mouth region reconstruction tasks, respectively. Each of these tasks corresponds to distinct 0-1 sequence design patterns.

### Multi-Modal Decoupled Cross-Attention

Given  $z$  as the input of Multi-Modal Decoupled Cross-Attention, the audio, text and image embeddings are injected in Multi-Modal Decoupled Cross-Attention as follows:

$$z_o = z + CA(Q(z), (KV_t(c_t) + KV_i(c_i) + KV_a(c_a) * d(c_t, c_i, c_a))) \quad (2)$$

Specifically, the text, audio, and image prompts are encoded by umT5, an audio extractor, and CLIP, respectively, into text embeddings  $c_t$ , audio embeddings  $c_a$ , and image embeddings  $c_i$ . These embeddings are then injected into DiT via cross-attention. In the Multi-Modal Decoupled Cross-Attention module, we adopt a decoupled mechanism similar to IP-Adapter. Specifically, we project the embeddings from different modalities separately as keys and values while sharing the same query for performing text, audio, and image cross-attention. The outputs from the three cross-attention operations are then fused by summation.

**Frame-Audio Aligned Injection.** In earlier works, U-Net served as the foundational model for audio-driven human animation, where each latent frame was temporally aligned with the audio token one by one. As a result, only spatial attention mechanisms were required to maintain synchroniza-



Figure 3: Qualitative comparison with SOTA methods for talking human animation.

tion between audio and video. However, due to the temporal downsampling ratio  $r$  introduced by the VAE in DiT, a single latent frame corresponds to  $r$  audio feature tokens along the temporal dimension.

To this end, we adopt an audio segmentation strategy to achieve temporal alignment between audio features and latent frames, followed by implementing latent frame-wise cross-attention. Given the audio input  $c_a$ , we utilize Whisper-Tiny  $E_a$  to extract audio features and employ an MLP as an audio projection module to align the dimensions of the inputs to the DiT blocks. Let the audio embeddings be denoted as  $\{c_a^1, c_a^2, \dots, c_a^{t_a}\}$ , where  $t_a$  represents the length of the audio sequence. The audio embeddings are evenly divided into segments, each containing  $r \times \alpha$  features, where  $\alpha$  denotes the number of audio embedding features corresponding to the duration of one video frame.

Next, we identify the center feature of each segment over its duration, denoted as  $\{c_a^{m_1}, c_a^{m_2}, \dots, c_a^{m_\tau}\}$ , where  $\tau$  is the temporal length of the latent. To ensure smooth transitions between segments, we extend both forward and backward by  $r + e$  features from each center feature, resulting in latent frame-wise audio embedding segments  $\{s_a^1, s_a^2, \dots, s_a^\tau\}$ , where  $e$  represents the overlap added for smoothness.

For audio-latent alignment, we perform latent frame-wise local cross-attention over each corresponding audio embedding segment. This approach ensures precise temporal correspondence while maintaining computational efficiency.

### Multi-Modal Phase-specific Drop

In the Multi-Modal Decoupled Cross-Attn module, simultaneously injecting all modals (text, audio, and image) usually causes the model to undergo a process of initial degradation

followed by eventual convergence, which diminishes the effectiveness of the pretrained model. Inspired by the PhD Loss in EchoMimicV2 (Meng et al. 2025), we divided the denoise time-steps (ranging from 1000 to 1) into early, middle, and late phases, based on the scale of noise addition. In the early phase, following the principles of EchoMimicV2, we prioritize larger motions and structural features. Thus, we activate the Text Cross-Attn, which contains prompts of body movements, while dropping out the other image and audio modalities injection; In the middle phase, we introduce the Audio and Image Cross-Attn to refine the model’s learning; In the late phase, we randomly drop 1 to 2 modalities to enhance the control capability of individual modalities. Note that we uniformly sample timesteps from all three phases in each iteration to ensure the training balance.

### Training Strategy

Our training pipeline adopts an alternating strategy that combines Supervised Fine-Tuning (SFT) with Direct Preference Optimization (DPO). During the SFT phase, we incrementally introduce DPO-guided preference learning to optimize hand details and refine facial expressions. By embedding DPO seamlessly into the broader SFT framework, this training approach preserves the model’s generalization capacity while effectively addressing issues such as hallucination and artifact generation. Moreover, it leads to significant enhancements in the finer aspects of the generated outputs.

Talking Head						
methods	Sync-C $\uparrow$	Sync-D $\downarrow$	FID $\downarrow$	FVD $\downarrow$	IQA $\uparrow$	ASE $\uparrow$
EchoMimicV3	4.78	9.62	41.83	430.79	4.38	2.69
w/o Multi-Modal PhD	4.76	9.68	41.03	603.95	4.09	2.63
w/o DPO	4.07	11.12	41.87	600.98	4.23	2.11
w/o Multi-Task Learning	4.45	10.34	41.76	594.76	4.37	2.67
Talking Human						
EchoMimicV3	4.39	8.51	42.45	496.76	4.63	3.20
w/o Multi-Modal PhD	4.30	9.01	43.20	510.08	4.56	3.23
w/o DPO	4.02	11.2	45.98	523.75	4.07	2.98
w/o Multi-Task Learning	4.13	9.37	41.98	489.65	4.54	3.02

Table 1: Quantitative results for EchoMimicV3.

## Experiments

### Experimental Setups

**Implementation.** To train EchoMimicV3, we utilize Wan2.1-FUN-inp-480p-1.3B<sup>1</sup> as the foundational model.

The input video length is set to 113. The classifier-free guidance for text is set to 2 and classifier-free guidance for audio is set to 9. The training process is conducted on 64 96GB GPUs, with a learning rate set to 1e-4. For efficiency, we first extract the VAE latents and caption embeddings for all the training data.

**Dataset.** We train our model using a combination of open-source data and proprietary data. The open-source datasets we utilize include the EchoMimicV2 dataset, the HDTF dataset, as well as our self-collected data. To ensure data quality, we apply filtering techniques such as audio synchronization and subtitle removal. The total amount of data used for training is approximately 1,500 hours.

**Metrics.** To comprehensively evaluate the performance of our model, we utilize the Fréchet Inception Distance (FID) (Deng et al. 2019) as a metric for assessing the fidelity and visual quality of generated images. For video generation tasks, we adopt the Fréchet Video Distance (FVD) (Unterthiner et al. 2018) to measure the temporal coherence and overall quality of synthesized videos. In addition, we analyze both perceptual quality (IQA) and aesthetic appeal (ASE) of the generated content. To further examine the alignment between audio and visual modalities, particularly in lip-sync generation, we employ the Sync-C and Sync-D metrics (Prajwal et al. 2020), which provide robust evaluations of synchronization accuracy.

### Results

**Results on Talking Face.** We present both qualitative and quantitative comparison results with several existing talking face methods, including EchoMimic (Chen et al. 2025c), Hallo3 (Cui et al. 2024), FantasyTalking (Wang et al. 2025), HunyuanAvatar (Chen et al. 2025b) and OmniAvatar (Xu et al. 2023). As shown in Figure 3, the qualitative comparison demonstrates that our method achieves higher naturalness in facial expressions compared to non-DiT approaches. When contrasted with DiT-based methods, our

model uses only approximately one-tenth of the parameter count while achieving comparable performance to these large-scale models, highlighting the effectiveness and efficiency of our approach. Notably, in terms of lip-sync alignment, our solution surpasses some methods with over 10 billion parameters. Regarding identity preservation, even without incorporating additional ID injection modules, our method matches the performance of certain large models (10B+ parameters) that utilize dedicated identity preservation mechanisms.

In the quantitative evaluation, we randomly select 50 samples from EchoMimicV3 generated videos. We employ metrics including FID, FVD, Sync-C, IQA, ASE, and motion smoothness. These metrics comprehensively assess the generation quality, lip-sync accuracy, video fidelity, and aesthetic appeal of our approach. The results in Table X indicate that our method performs on par with other state-of-the-art techniques in terms of FID and FVD. For lip-sync alignment, our approach is comparable to specialized digital human solutions and outperforms prominent methods such as FantasyTalk and OmniAvatar, despite being significantly more parameter-efficient. **Results on Upper-Body Human Animation.**

We conducted both qualitative and quantitative comparisons with existing methods for half-body digital human generation. These include EchoMimicV2 (Meng et al. 2025), HunyuanAvatar (Chen et al. 2025b), OmniHuman (Lin et al. 2025), and OmniAvatar (Xu et al. 2023). As shown in Tab ??, our method demonstrates significant improvements in key aspects such as gesture accuracy, background preservation, facial expressions, lip-sync alignment, and motion smoothness when compared to non-DiT approaches like EchoMimicV2. Furthermore, our approach exhibits strong competitiveness against models with over 10 billion parameters, including FantasyTalk and Hallo3, despite being significantly smaller in size.

In terms of identity preservation (ID retention), our solution surpasses FantasyTalk, achieving more consistent and natural results across different scenarios. For cartoon-style applications, our method achieves performance on par with state-of-the-art approaches such as HunyuanAvatar and FantasyTalk, demonstrating its versatility and robustness. Ad-

<sup>1</sup> <https://github.com/aigc-apps/VideoX-Fun>



Figure 4: EchoMimicV3 can cover various scenarios, such as podcast, karaoke, cartoon style and so on.

ditionally, as highlighted in the quantitative analysis, our model outperforms non-DiT baselines in video quality, lip-sync precision, and motion fluidity. Notably, it even matches or exceeds the performance of methods with parameter counts ten times larger than ours, underscoring the efficiency and effectiveness of our design.

These results highlight that EchoMimicV3 achieves competitive performance with only a fraction (approximately one-tenth) of the parameters required by current state-of-the-art methods. This not only showcases its ability to generate high-quality digital humans but also emphasizes its strong generalization capabilities across diverse scenarios, including blog-style videos, singing performances, and cartoon animations.

To further validate the robustness of our approach, we performed quantitative comparisons across a variety of scenarios, including blog-style videos, singing performances, and cartoon animations. As summarized in Tab. ??, our method consistently surpasses non-DiT models in generation quality, video fidelity, lip-sync accuracy, and motion

smoothness. Notably, despite being significantly smaller in size (e.g., having 10 times fewer parameters), our method performs on par with or even outperforms many state-of-the-art models with over 10 billion parameters, such as FantasyTalk. These findings underscore that EchoMimicV3 achieves highly competitive performance in digital human generation while utilizing only one-tenth of the parameters required by current SOTA models. Additionally, our method demonstrates strong generalization capabilities across multiple scenarios, highlighting its versatility and efficiency.

## Ablation Studies

**Ablation on Multi-Modal Phase-specific Dropout.** We conduct ablation experiments on the Multi-Modal Phase-specific Dropout module. The evaluation is performed using quantitative metrics, including FVD, Sync-C, IQA, and the number of iterations. As shown in the table ??, the first row presents the results without incorporating this module. Although there is a general decrease in performance across all metrics, the convergence speed is significantly reduced.

Talking Head		
methods	time-steps	inference decay
EchoMimicV3	5	1min
FatasyTalk	25	18min
HunyuanAvatar	25	17min
Talking Human		
EchoMimicV3	25	4min
FatasyTalk	25	18min
HunyuanAvatar	25	17min

Table 2: Inference speed for 5s videos on single A100 GPU.

**Ablation on Multi-Task Learning.** We experimentally validate the performance of multi-task training and single-task training after removing the mouth replacement and the first-and-last frame reference tasks. As shown in the table, our approach enables mutual enhancement among multiple tasks. Notably, there is a progressive relationship in difficulty between the mouth replacement and upper-body generation tasks, which facilitates faster convergence of the model.

## Related Work

### Video Generation

Early research in video generation primarily focused on 2D U-Net architectures and motion modules, which were subsequently extended to 3D frameworks. The introduction of spatiotemporal convolutions marked a pivotal advancement, enabling models such as SVD to generate short video clips with exceptional spatial fidelity. Building upon these foundational developments, diffusion-based models like DiT have progressively gained prominence in visual generation tasks. These models harness the reduced inductive bias and non-local properties of self-attention mechanisms, leading to notable improvements in temporal coherence and motion fluidity during video synthesis.

Further innovations in text-to-video generation have been driven by frameworks such as CogVideo (Yang et al. 2024b) and Goku (Chen et al. 2025a), which integrate large-scale vision-language pretraining with hierarchical token fusion strategies. These approaches achieve precise semantic alignment between textual prompts and generated content, enabling fine-grained control over video outputs. Hunyuan-Video (Kong et al. 2024) has expanded this research direction by embedding multimodal prompts into a dual-stream DiT architecture, facilitating robust conditional control across varied and complex scenarios. Additionally, Wan (Wan et al. 2025) has introduced a suite of large-scale video generation models characterized by remarkable scalability and state-of-the-art performance, establishing new benchmarks for the field and demonstrating the potential for broader applications in video synthesis.

### Talking Human Animation

The objective of audio-driven human animation is to synthesize natural and expressive gestures from speech audio, ensuring that the generated motion aligns seamlessly with the input in terms of semantics, emotional tone, and temporal rhythm. While prior research has predominantly focused on

animating talking heads (Zhu et al. 2024; Xu et al. 2024b), recent advancements have introduced innovative techniques to enhance the quality and consistency of such animations. For instance, EMO (Tian et al. 2024) incorporates a Frame Encoding module to maintain temporal coherence, while AniPortrait (Wei, Yang, and Wang 2024) leverages 3D facial structures mapped onto 2D poses to produce highly coherent sequences.

V-Express achieves precise synchronization between audio signals and lip movements, further refining the subtleties of emotional expression. Hallo (Xu et al. 2024a) employs diffusion models to provide enhanced control over both facial expressions and body poses, enabling more nuanced animations. Similarly, Vlogger (Zhuang et al. 2024) utilizes a diffusion-based framework to generate high-fidelity talking videos from a single input image, offering superior controllability and visual quality. MegActor (Yang et al. 2024a) integrates multimodal inputs—combining audio and visual cues—through a conditional diffusion transformer to achieve realistic portrait animations. In the domain of full-body gesture synthesis, TANGO (Liu et al. 2024) introduces a method for generating co-speech body gestures, improving alignment accuracy and reducing visual artifacts. EchoMimic (Chen et al. 2024) extends this capability by supporting flexible generation modes, allowing animations to be driven either by audio alone, facial pose sequences, or a hybrid combination of both. Furthermore, CyberHost (Lin et al. 2024) supports multimodal control signals, including audio, full-body keypoint maps, 2D hand pose sequences, and body movement trajectories, enabling versatile and precise animation across diverse scenarios. Based on video generation model, OmniHuman (Lin et al. 2025) uses multi-condition progressive dropout strategy to achieve SOTA performance. Hunyuanvideo-Avatar (Chen et al. 2025b) and MultiTalk (Sung-Bin et al. 2024) can use multi-audios to drive multi-character. Omniavatar (Xu et al. 2023) uses an efficient module to inject audio into the transformer. However, DiT-based audio-driven human animation methods still encounter substantial difficulties in achieving accurate lip synchronization and generating long-duration videos. These challenges remain prominent, indicating the need for further advancements in model design and training strategies.

## Conclusion

In this work, we propose an effective framework, EchoMimicV3, to master versatile multi-modal human animation tasks in a single 1.3B model. We propose a new multi-task paradigm, dubbed as Multi-Task Coupled Inpainting for multiple task joint training. Besides, we introduce Multi-Modal Decoupled Cross-Attn and Phase-specific Drop for text, audio, and image prompts effective injection. Furthermore, we introduce a new alternative training strategy to achieve vivid performance. Extensive experiments demonstrate that EchoMimicV3 remains competitive even when compared to models ten times its model scale.

## References

- Chen, S.; Ge, C.; Zhang, Y.; Zhang, Y.; Zhu, F.; Yang, H.; Hao, H.; Wu, H.; Lai, Z.; Hu, Y.; et al. 2025a. Goku: Flow Based Video Generative Foundation Models. *arXiv preprint arXiv:2502.04896*.
- Chen, Y.; Liang, S.; Zhou, Z.; Huang, Z.; Ma, Y.; Tang, J.; Lin, Q.; Zhou, Y.; and Lu, Q. 2025b. HunyuanVideo-Avatar: High-Fidelity Audio-Driven Human Animation for Multiple Characters. *arXiv preprint arXiv:2505.20156*.
- Chen, Z.; Cao, J.; Chen, Z.; Li, Y.; and Ma, C. 2024. Echomimic: Lifelike audio-driven portrait animations through editable landmark conditions. *arXiv preprint arXiv:2407.08136*.
- Chen, Z.; Cao, J.; Chen, Z.; Li, Y.; and Ma, C. 2025c. Echomimic: Lifelike audio-driven portrait animations through editable landmark conditions. In *Proceedings of the AAAI Conference on Artificial Intelligence*, volume 39, 2403–2410.
- Cui, J.; Li, H.; Zhan, Y.; Shang, H.; Cheng, K.; Ma, Y.; Mu, S.; Zhou, H.; Wang, J.; and Zhu, S. 2024. Hallo3: Highly dynamic and realistic portrait image animation with diffusion transformer networks. *arXiv e-prints*, arXiv–2412.
- Deng, Y.; Yang, J.; Xu, S.; Chen, D.; Jia, Y.; and Tong, X. 2019. Accurate 3d face reconstruction with weakly-supervised learning: From single image to image set. In *Proceedings of the IEEE/CVF conference on computer vision and pattern recognition workshops*, 0–0.
- Kingma, D. P. 2013. Auto-encoding variational bayes. *arXiv preprint arXiv:1312.6114*.
- Kong, W.; Tian, Q.; Zhang, Z.; Min, R.; Dai, Z.; Zhou, J.; Xiong, J.; Li, X.; Wu, B.; Zhang, J.; et al. 2024. Hunyuan-video: A systematic framework for large video generative models. *arXiv preprint arXiv:2412.03603*.
- Lin, G.; Jiang, J.; Liang, C.; Zhong, T.; Yang, J.; and Zheng, Y. 2024. CyberHost: Taming Audio-driven Avatar Diffusion Model with Region Codebook Attention. *arXiv preprint arXiv:2409.01876*.
- Lin, G.; Jiang, J.; Yang, J.; Zheng, Z.; and Liang, C. 2025. OmniHuman-1: Rethinking the Scaling-Up of One-Stage Conditioned Human Animation Models. *arXiv preprint arXiv:2502.01061*.
- Liu, H.; Yang, X.; Akiyama, T.; Huang, Y.; Li, Q.; Kuriyama, S.; and Taketomi, T. 2024. TANGO: Co-Speech Gesture Video Reenactment with Hierarchical Audio Motion Embedding and Diffusion Interpolation. *arXiv preprint arXiv:2410.04221*.
- Meng, R.; Zhang, X.; Li, Y.; and Ma, C. 2025. Echomimicv2: Towards striking, simplified, and semi-body human animation. In *Proceedings of the Computer Vision and Pattern Recognition Conference*, 5489–5498.
- Peebles, W.; and Xie, S. 2023. Scalable diffusion models with transformers. In *Proceedings of the IEEE/CVF international conference on computer vision*, 4195–4205.
- Prajwal, K.; Mukhopadhyay, R.; Namboodiri, V. P.; and Jawahar, C. 2020. A lip sync expert is all you need for speech to lip generation in the wild. In *Proceedings of the 28th ACM international conference on multimedia*, 484–492.
- Rombach, R.; Blattmann, A.; Lorenz, D.; Esser, P.; and Ommer, B. 2022. High-resolution image synthesis with latent diffusion models. In *Proceedings of the IEEE/CVF conference on computer vision and pattern recognition*, 10684–10695.
- Sung-Bin, K.; Chae-Yeon, L.; Son, G.; Hyun-Bin, O.; Ju, J.; Nam, S.; and Oh, T.-H. 2024. MultiTalk: Enhancing 3D Talking Head Generation Across Languages with Multilingual Video Dataset. *arXiv preprint arXiv:2406.14272*.
- Tian, L.; Wang, Q.; Zhang, B.; and Bo, L. 2024. Emo: Emote portrait alive-generating expressive portrait videos with audio2video diffusion model under weak conditions. *arXiv preprint arXiv:2402.17485*.
- Unterthiner, T.; Van Steenkiste, S.; Kurach, K.; Marinier, R.; Michalski, M.; and Gelly, S. 2018. Towards accurate generative models of video: A new metric & challenges. *arXiv preprint arXiv:1812.01717*.
- Vaswani, A.; Shazeer, N.; Parmar, N.; Uszkoreit, J.; Jones, L.; Gomez, A. N.; Kaiser, Ł.; and Polosukhin, I. 2017. Attention is all you need. *Advances in neural information processing systems*, 30.
- Wan, T.; Wang, A.; Ai, B.; Wen, B.; Mao, C.; Xie, C.-W.; Chen, D.; Yu, F.; Zhao, H.; Yang, J.; et al. 2025. Wan: Open and advanced large-scale video generative models. *arXiv preprint arXiv:2503.20314*.
- Wang, M.; Wang, Q.; Jiang, F.; Fan, Y.; Zhang, Y.; Qi, Y.; Zhao, K.; and Xu, M. 2025. Fantasytalking: Realistic talking portrait generation via coherent motion synthesis. *arXiv preprint arXiv:2504.04842*.
- Wei, H.; Yang, Z.; and Wang, Z. 2024. Aniportrait: Audio-driven synthesis of photorealistic portrait animation. *arXiv preprint arXiv:2403.17694*.
- Xu, H.; Song, G.; Jiang, Z.; Zhang, J.; Shi, Y.; Liu, J.; Ma, W.; Feng, J.; and Luo, L. 2023. Omniavatar: Geometry-guided controllable 3d head synthesis. In *Proceedings of the IEEE/CVF Conference on Computer Vision and Pattern Recognition*, 12814–12824.
- Xu, M.; Li, H.; Su, Q.; Shang, H.; Zhang, L.; Liu, C.; Wang, J.; Yao, Y.; and Zhu, S. 2024a. Hallo: Hierarchical audio-driven visual synthesis for portrait image animation. *arXiv preprint arXiv:2406.08801*.
- Xu, S.; Chen, G.; Guo, Y.-X.; Yang, J.; Li, C.; Zang, Z.; Zhang, Y.; Tong, X.; and Guo, B. 2024b. Vasa-1: Lifelike audio-driven talking faces generated in real time. *Advances in Neural Information Processing Systems*, 37: 660–684.
- Yang, S.; Li, H.; Wu, J.; Jing, M.; Li, L.; Ji, R.; Liang, J.; Fan, H.; and Wang, J. 2024a. MegActor-Σ: Unlocking Flexible Mixed-Modal Control in Portrait Animation with Diffusion Transformer. *arXiv preprint arXiv:2408.14975*.
- Yang, Z.; Teng, J.; Zheng, W.; Ding, M.; Huang, S.; Xu, J.; Yang, Y.; Hong, W.; Zhang, X.; Feng, G.; et al. 2024b. Cogvideox: Text-to-video diffusion models with an expert transformer. *arXiv preprint arXiv:2408.06072*.

Zhu, S.; Chen, J. L.; Dai, Z.; Dong, Z.; Xu, Y.; Cao, X.; Yao, Y.; Zhu, H.; and Zhu, S. 2024. Champ: Controllable and consistent human image animation with 3d parametric guidance. In *European Conference on Computer Vision*, 145–162. Springer.

Zhuang, S.; Li, K.; Chen, X.; Wang, Y.; Liu, Z.; Qiao, Y.; and Wang, Y. 2024. Vlogger: Make your dream a vlog. In *Proceedings of the IEEE/CVF Conference on Computer Vision and Pattern Recognition*, 8806–8817.